

The biogenic silica variation and paleoproductivity evolution in the eastern Indian Ocean during the past 20 000 a

Yonghang Xu^{1*}, Liang Wang¹, Zhikun Lai¹, Xiaohui Xu¹, Feng Wang¹, Shengfa Liu^{2,3}, Xuefa Shi^{2,3}, Rainer Arief Troa⁴, Rina Zuraida⁵, Eko Triarso⁴, Marfasran Hendrizen⁶

¹Laboratory of Ocean and Coast Geology, Third Institute of Oceanography, Ministry of Natural Resources, Xiamen 361005, China

²Laboratory for Marine Geology, Pilot National Laboratory for Marine Science and Technology (Qingdao), Qingdao 266237, China

³Key Laboratory of Marine Sedimentology and Environmental Geology, First Institute of Oceanography, Ministry of Natural Resources, Qingdao 266061, China

⁴Marine Research Center, Agency of Research and Human Resources for Marine and Fisheries, Jakarta 14420, Indonesia

⁵Marine Geological Institute, Agency for Research and Development for Energy and Mineral Resources, Bandung 40174, Indonesia

⁶Research Center for Geotechnology, Indonesia Institute of Sciences, Bandung 40135, Indonesia

Received 27 October 2017; accepted 6 February 2018

© Chinese Society for Oceanography and Springer-Verlag GmbH Germany, part of Springer Nature 2019

Abstract

The biogenic silica of sediment samples from Core CJ01-185 which is collected from the eastern India Ocean off the Sunda Strait is analyzed to evaluate the impact of the opening of the Sunda Strait on a paleoproductivity evolution. The new results indicate that the biogenic silica mass values of Core CJ01-185 show the lowest 0.86% in the last glacial period, and reach its maxima of 1.89% in the late Holocene. Furthermore, the biogenic silica mass accumulation rate (MAR_{BSi}) values also vary with much higher during the late Holocene than during the last glaciation. The input of additional terrigenous materials from the Java Sea has enhanced the paleoproductivity and increased the biogenic silica mass and MAR_{BSi} values after the opening of the Sunda Strait. It is suggested that the paleoproductivity in the study area is mainly influenced by the southeast monsoon and upwelling before the opening of the Sunda Strait. However, the paleoproductivity is dominated by the terrigenous materials input other than by the southeast monsoon or upwelling in the Holocene.

Key words: biogenic silica, paleoproductivity, Sunda Strait, eastern India Ocean

Citation: Xu Yonghang, Wang Liang, Lai Zhikun, Xu Xiaohui, Wang Feng, Liu Shengfa, Shi Xuefa, Troa Rainer Arief, Zuraida Rina, Triarso Eko, Hendrizen Marfasran. 2019. The biogenic silica variation and paleoproductivity evolution in the eastern Indian Ocean during the past 20 000 a. Acta Oceanologica Sinica, 38(1): 78–84, doi: 10.1007/s13131-019-1372-z

1 Introduction

Biogenic silica (BSi) which is mostly composed of siliceous plankton (such as diatom, radiolarian and sponge spicule remains), is a major biogenic component of marine sediments. Of these groups of siliceous plankton, diatoms account for the most BSi production. Diatoms are particularly in high-latitude areas and along some continental margins, especially in upwelling areas (De Wever et al., 2002; Karleskint et al., 2012). More than 40% of the global primary production is attributable to diatoms, suggesting a close coupling of the ocean's silica and carbon cycles (Nelson et al., 1995). Therefore, changes in a BSi abundance in sedimentary record is a potentially important paleoproductivity proxy (DeMaster, 1991; Ragueneau et al., 1996; Ragueneau et al., 2000).

The eastern Indian Ocean (EIO) is the important pathway of heat transfer from the Western Pacific Warm Pool to the Indian Ocean (Qu et al., 2005; Sprintall et al., 2014). The upwelling sys-

tem along the Sumatra-Java coast is associated with the monsoon climate (Fig. 1). The upwelling-related high primary productivity was a major control factor for the observed high carbon and nitrogen contents of surface sediments off southeast Java (Susanto et al., 2001) (Figs 2a and b).

In this study, we present a continuous, high-resolution record from Core CJ01-185 collected from eastern India Ocean off the Sunda Strait, and now carried out the biogenic silica and the biogenic silica flux over the past ca. 19 500 a. We attempt to seek a correlation that may inherently exist between biogenic silica and a paleoenvironment condition and the influence of the paleoproductivity evolution before and after the opening of the Sunda Strait.

2 Background of the study area

The Sunda Shelf between the Indonesian Archipelago and Viet Nam, is one of the largest shelves and has a water depth of

Foundation item: The National Programme on Global Change and Air-sea Interaction under contract Nos GASI-GEOGE-06-03 and GASI-02-IND-CJ01; the China-Indonesia Joint Project under contract No. "BENTHIC"; the Third Institute of Oceanography, Ministry of Natural Resources Research Grant under contract No. 2015015.

*Corresponding author, E-mail: xuyonghang@tio.org.cn

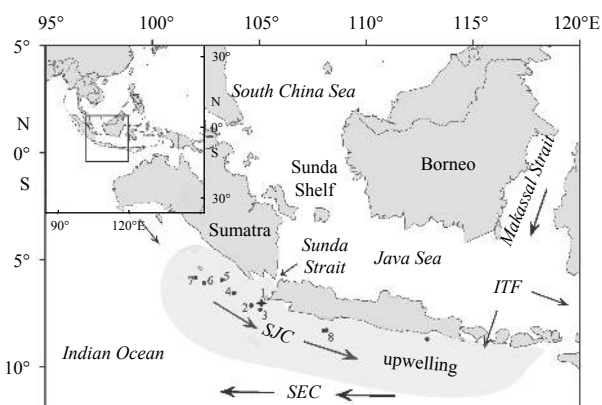


Fig. 1. Position of Core CJ01-185 (1, black star) with oceanographic currents (solid arrows). Location of Core GeoB 10042-1 (2) and GeoB 10043-3 (3) (Setiawan et al., 2015), Core SO139-74KL (4, Lückge et al., 2009), Core GeoB 10038-4 (5, Romero et al., 2012), Core BAR9442 (6, Gingele et al., 2002), Core BAR9403 (7, Murgese et al., 2008). ITF represents Indonesian Throughflow, SEC South Equatorial Current and SJC South Java Current.

less than 70 m. The Sunda Shelf was exposed during the last glacial maximum, when the sea level was approximately -130 m lower than today (Hanebuth et al., 2000). With the increase in the sea level, the Sunda Shelf was flooded because the water depth increased to -20 m at 9.5 ka (Hanebuth et al., 2000, 2011; Setiawan et al., 2015). The Sunda Strait connects the Java Sea and the EIO (Fig. 1). The hydrologic conditions of the EIO were influenced by warmer and low-salinity sea water, which is from the Java Sea entered the EIO with the Indonesian Throughflow through the Sunda Strait (Xu et al., 2008; Linsley et al., 2010). Setiawan et al. (2015) proposed that the sea surface temperatures increased approximately 1.7°C after the opening of the Sunda Strait at approximately 10 ka.

The South Java current which is characterized by low salinity and warm water generally flows eastward along the coasts of Sumatra and Java (Sprintall et al., 2010). As the southeast monsoon strengthens, the South Java current turns to westward and merges with the south equatorial current in September. Cool and fresh water was transported into the Indian Ocean by the Indonesian throughflow (Gordon et al., 2003; Talley and Sprintall, 2005). Gordon (2005) suggested that the upper water body structure and the sea surface temperatures in the EIO were influenced by the Indonesian Throughflow.

The southeast (Australian) and northwest (Indonesian) monsoons are important climate systems in the EIO. The southeast monsoon is associated with a dry weather and little rainfall from May to September (Fig. 2e). However, from November to March, the northwest monsoon strengthens, carrying large amounts of moisture to the Java region (Fig. 2e), which may be due to the southward migration of the Intertropical Convergence Zone (ITCZ) (Qu et al., 2005).

The upwelling along the Java-Sumatra Indian Ocean coasts is a response to regional winds associated with the monsoon climate. Susanto et al. (2001) suggested that the upwelling with a low sea surface temperature and a high salinity was most intense southern of Java in July and southwest of Sumatra in October (Figs 2c and d). The eastern Indian Ocean is significantly influenced by the ENSO. A significant interannual variability of the Java-Sumatra upwelling is also linked to the ENSO through the Indonesian throughflow. During El Niño (La Niña), the ITF car-

ries colder (warmer) water shallowing (deepening) thermocline depth and enhancing (reducing) upwelling strength (Susanto et al., 2001).

3 Samples and analytical methods

A sediment Core CJ01-185 was collected from off the Sunda Strait (7°1'17.28"S, 105°6'11.27"E, 1 538 m water depth, core length 300 cm) with R/V *GEOMARIN III* in 2014 (Fig. 1). There are two tephra layers (3–5 and 47–55 cm layers) in this sediment core (Xu et al., 2017). The sand content in this core is about 3%, and the silt content is 74%, the clay content is 23% (Xu et al., 2017) (Fig. 3). The silt content has significantly increase since 4.2 ka, and mean grain size also increases (Fig. 3).

Core CJ01-185 was sampled every 1 cm, and 91 samples for BSi analyses. Dissolved silica in the extractions was determined using a molybdate blue spectrophotometric method (Mortlock and Froelich, 1989). Samples were dried and ground to 200 mesh in an agate grinder. Then, about 130 mg of sediment was put into a 50 mL polypropylene centrifuge tube; 1 mol/L HCl and 10% H₂O₂ were added to remove the carbonate and organics, and then 2 mol/L Na₂CO₃ solution was added, and the sample placed in a water bath preheated to 85°C. After that, 125 μL of the supernatant was taken after 1, 2, 3, 4, 5 and 6 h of centrifugation. More detail could be seen in Wang et al. (2014). The mass percent of extracted silica was plotted versus time, and the extrapolated intercept equals the BSi content of the sample (DeMaster, 1981). The precision of BSi content was better than ±3%. The analyses of BSi content were carried out in the Ocean University of China.

The calculation of BSi mass accumulation rates [MAR_{BSi} , g/(cm²·ka)] for the productivity proxies used linear sedimentation rates (LSR , cm/ka) and a dry bulk density (ρ) as follows: $MAR_{BSi} = X \times \rho \times LSR$ (Schoepfer et al., 2015). An age model of core CJ01-185 has previously been studied by Xu et al. (2017). We also collected the data of the dry bulk density, grain size and TOC content values (Xu et al., 2017) to present the paleoproductivity evolution.

4 Results

The BSi values of core CJ01-185 show lowest in the last glacial period, and increased from bottom upward (Fig. 3). On the basis of variations in the BSi content, we subdivided core into three units: the average BSi value is 0.86% in Unit 1 (19.5–10 ka), the average value is 1.48% in Unit 2 (10–4.2 ka) and 1.89% in Unit 3 (4.2 ka to present) (Figs 3 and 4).

The MAR_{BSi} over the past ca. 20 ka also increased from bottom upward. The MAR_{BSi} were lower than 5 g/(cm²·ka) between ca. 11 and 20 ka. From ca. 11 ka to 3.5 ka, the MAR_{BSi} increased gradually, and reached its higher value of 20 g/(cm²·ka). During the episode of ca 3.5 ka to 2.0 ka, the MAR_{BSi} reached its highest value with an average of 56 g/(cm²·ka). The MAR_{BSi} fluctuated within a narrow range of 20.9 to 25.7 g/(cm²·ka) from ca. 2 ka to present.

5 Discussion

The content of BSi is significantly affected by the sediment grain size, similar to other elements, such as organic carbon content (Bergamaschi et al., 1997; Lin et al., 2002; Wang et al., 2009). For example, the coarse grain fractions could dilution effects to BSi concentrations (Bernárdez et al., 2005). Wang et al. (2014) observed the BSi contents of different size fractions varied significantly in the East China Sea, with the mean grain size less than 16 μm, which is approximately 1.1 to 1.8 times that in bulk sediments. To limit the influence of the grain size, Bernárdez et al. (2005) suggested using BSi from the muddy fraction as an accur-

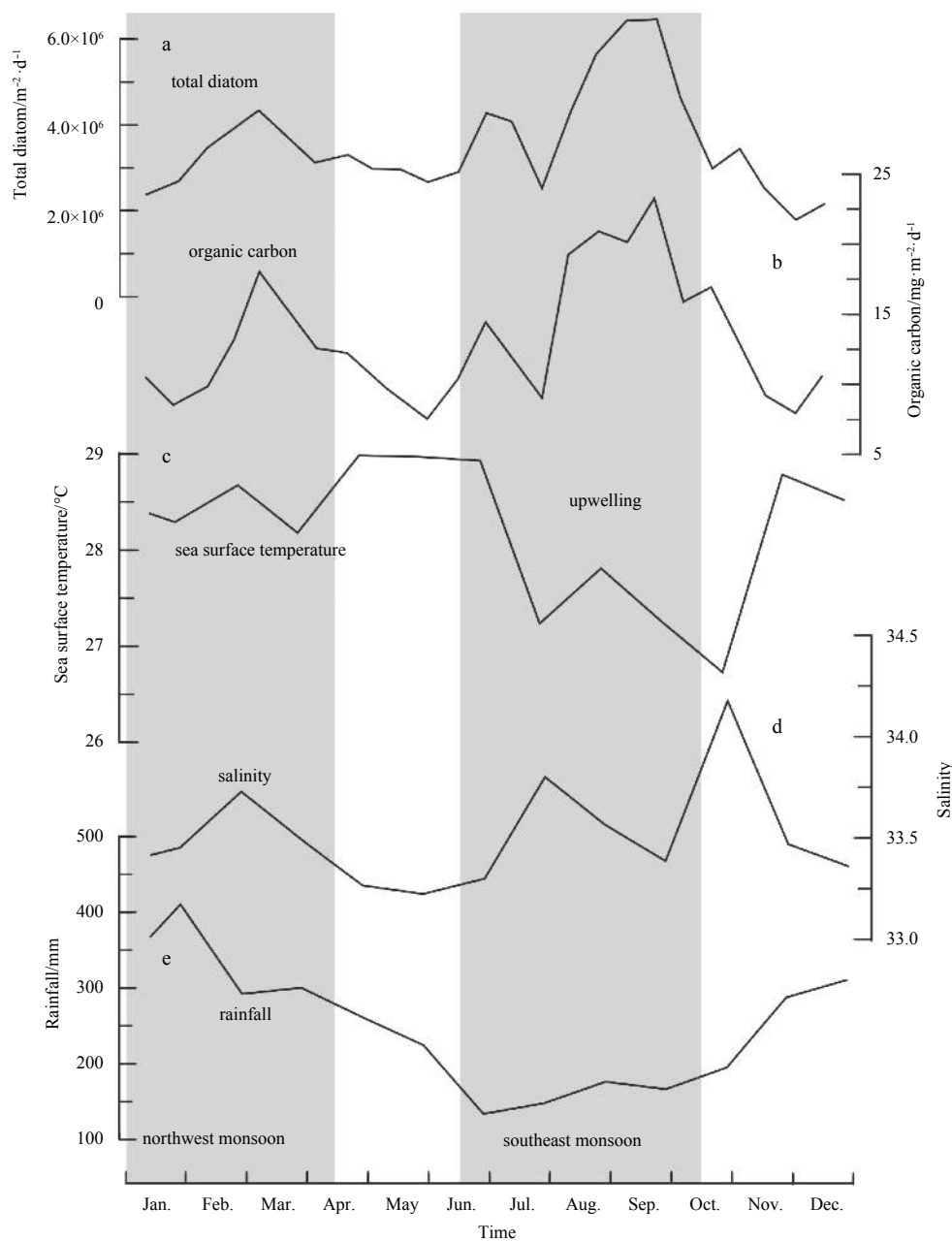


Fig. 2. Monsoon, average rainfall and upwelling in the IEO. Diatom (a) and organic carbon fluxes (b) are averaged for the sampling period between November 2000 and July 2003 at the JAM site off southern Java (Romero et al., 2009). Sea surface temperatures (c) and salinity (d) in the study region data from Levitus and Boyer (1994); average rainfall (e) of 214 months between 1951 and 1976 at weather station Batu Raja (Lückge et al., 2009).

ate paleoproductivity proxy. The mean grain size of Core CJ01-185 ranges from 5.54 to 12.2 μm , with an average of 8.57 μm , which is muddy fraction characteristic. In many cases, the BSi and TOC contents decrease with the increasing of the grain size. However, the BSi and TOC contents of Core CJ01-185 have significantly increased since 4.2 ka, accompanied by an increase in the mean grain size. Moreover, there are no correlation between BSi content and the mean grain size (Fig. 4), allowing us to use BSi content to as an important paleoproductivity proxy.

Our study reveals that the BSi content and MAR_{BSi} in Unit 1 gradually increased from the last glacial period to the early Holocene (Figs 3 and 5). The trends in the TOC and BSi generally compare well (Figs 5a and b). The *Globigerina bulloides* content

could be used as a proxy for the southeast monsoon and the upwelling intensity (Mohtadi et al., 2011). From the last Glacial Maximum to early Holocene, the high percentage (~30%) of *Globigerina bulloides* off Java Island was caused by strengthening of the southeast monsoon and upwelling (Fig. 5g) (Mohtadi et al., 2011). Furthermore, greater differences ($\Delta\delta^{18}\text{O}$) implied an intensified southeast monsoon and stronger upwelling during the early Holocene (Fig. 5g). The content of *Globigerina bulloides* also increased significantly in the BAR 9442 core during the period of 17–8 ka (Zhao and Ding, 2011). The total cyst concentrations and *O. centrocarpum* content in core BAR 9403 show an increase from 20 to 10 ka (Fig. 5e).

The BSi content in Unit 2 shows a rapid enrichment to an av-

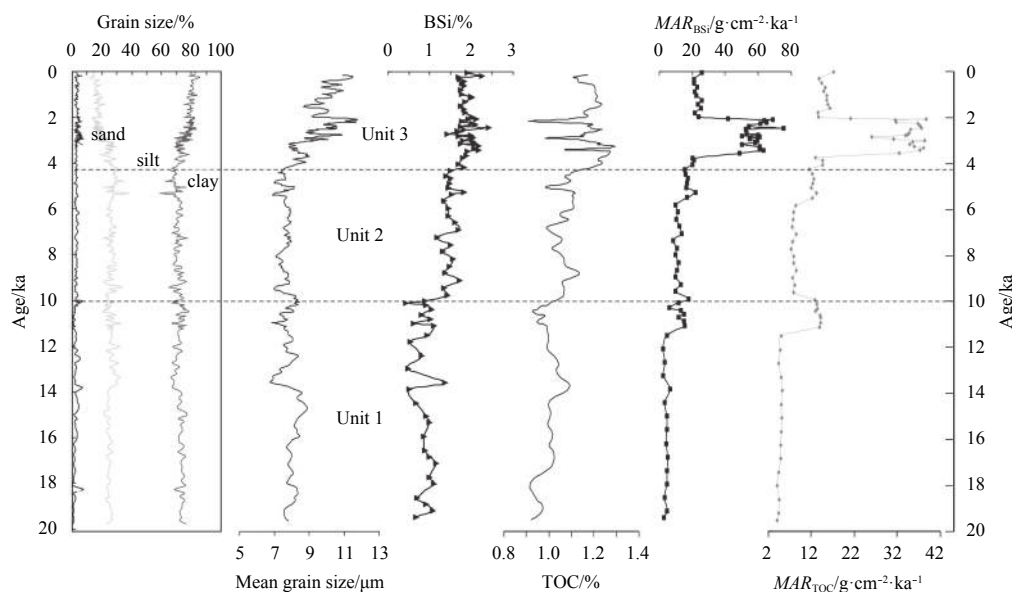


Fig. 3. Downcore variations of grain size populations and mean grain size, BSi content, TOC content, and mass accumulation rates of Core CJ01-185.

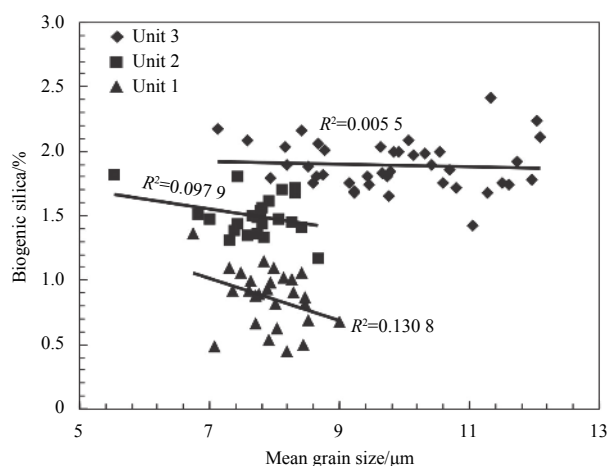


Fig. 4. Correlations between the BSi content and the mean grain size.

erage of 1.48% that is simultaneous with an increase in the MAR_{BSi} and the TOC values. These increases reflect higher paleoproductivity off the Sunda Strait. The maxima total diatom concentration of Core GeoB 10038-4 from the late deglaciation into the Holocene was also reported (Romero et al., 2012). Furthermore, the covariation of the total diatom concentration corresponds well with the seasonal monsoon and the strengthening and weakening phases of upwelling along the southern coast of Sumatra. These suggest a direct response of the diatom productivity and the upwelling intensity to the boreal summer insolation (Romero et al., 2012). Other scholars have also reported that the higher paleoproductivity in the Holocene than that in the late glacial period according organic carbon in Core SO139-74KL outside the Sunda Strait (Lückge et al., 2009).

The southeast monsoon was associated with the summer insolation (Figs 5g and i), and the strongest southeast monsoon was in response to the strongest insolation during the early Holocene (Mohtadi et al., 2011). The southeast monsoon has gradu-

ally weakened since the early Holocene (Fig. 5g), thereby leading to decreased upwelling and paleoproductivity off southern Java (Mohtadi et al., 2011). The total diatom concentration of Core GeoB 10038-4 decreased from the late Holocene (Romero et al., 2012). These declines reflect that the diatom paleoproductivity is lower during the late Holocene on southern coast of Sumatra. However, the BSi and MAR_{BSi} of Core CJ01-185 reached their maxima in Unit 3 during the late Holocene. In addition, the *G. bulloides* $\delta^{18}O$ and the total cyst concentrations in core BAR 9403 reached maximum in the late Holocene (Figs 5d and e). The *G. bulloides* $\delta^{18}O$ value of nearby core GeoB 10042-1 and GeoB 10043-3 also indicated the higher paleoproductivity in the late Holocene off the Sunda Strait (Setiawan et al., 2015).

The good correspondence between paleoproductivity and the solar insolation during the past 300 a in the EIO region is similar to seasonal upwelling off Sumatra and Java (Lückge et al., 2009). However, the paleoproductivity evolution in our study is not in agreement with variations in the solar insolation at a precessional frequency. On the basis of the maxima of the BSi and MAR_{BSi} from 4.2 ka to present, we speculate that the influx of terrigenous materials during the late Holocene might have acted as an additional source of nutrients delivered to the uppermost water column overlying Site CJ01-185. Our interpretation is also supported by the similar trends in global sea level variations (Fig. 5j) and the mean grain size at CJ01-185 (Xu et al., 2017). The mean grain size had been increased since the 4.2 ka (Fig. 3), which indicate that the input of terrigenous materials increased due to the monsoon rainfall. Although the southeast monsoon was relatively weakest, the northwest monsoon has strongest rainfall during the late Holocene (Mohtadi et al., 2011). Murgese et al. (2008) also suggested that the increasing presence of coastal species in Core BAR 9403 since 12 ka represented increased precipitation, river runoff and sediment discharge at sea.

The inputs of additional terrigenous nutrients from the Java Sea have enhanced paleoproductivity (Setiawan et al., 2015), although the southeast monsoon and the upwelling became weakened during the middle-late Holocene (Fig. 5g). The changes in the MAR_{BSi} , as well as the BSi and TOC contents in Holocene suggest

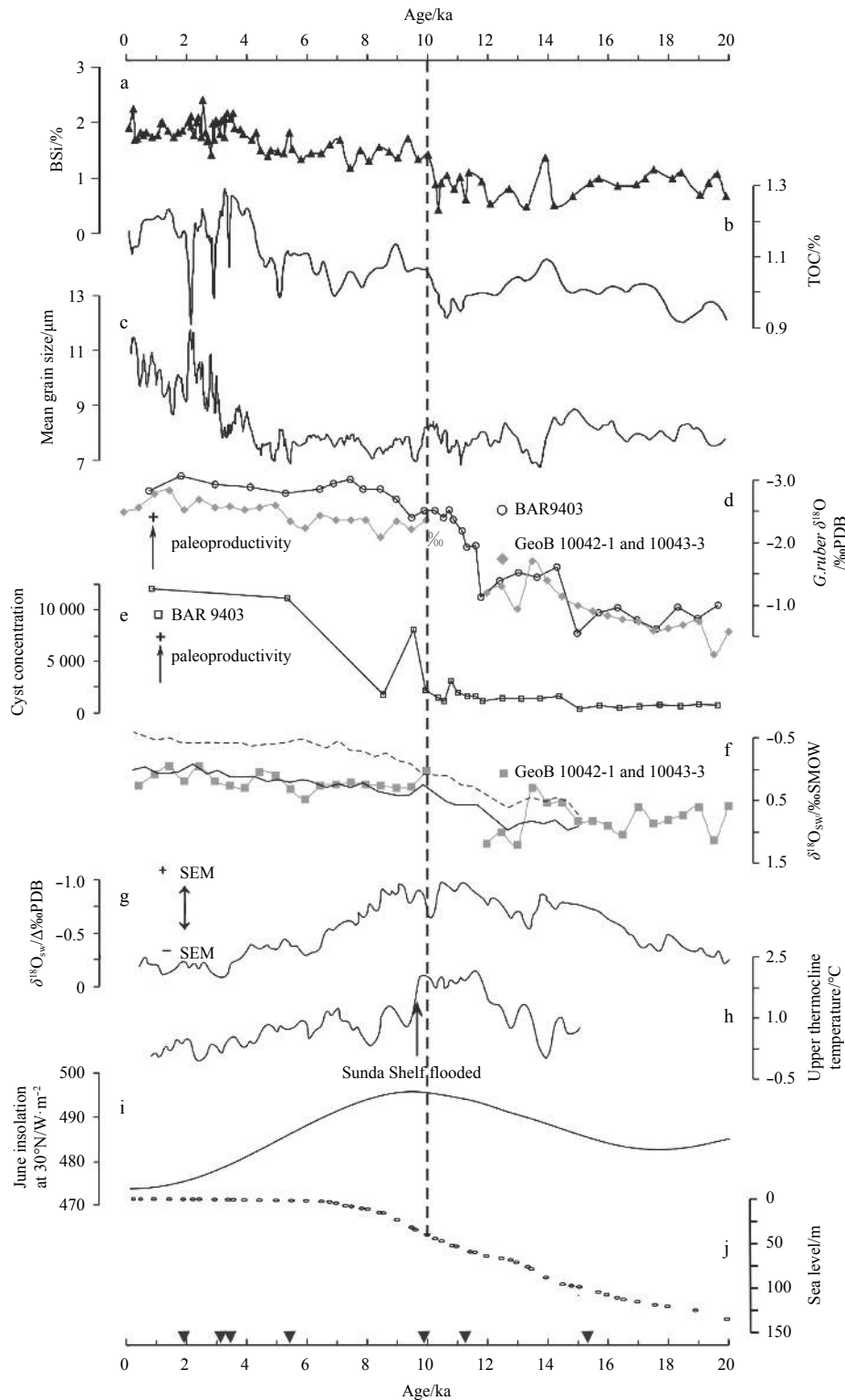


Fig. 5. Compare to the paleoclimate records in eastern Indian Ocean. a. BSi value for Core CJ01-185; b. total organic carbon (TOC) content for Core CJ01-185; c. mean grain size for Core CJ01-185; d. *G. ruber* $\delta^{18}\text{O}$ for Core BAR 9403 (Murgese et al., 2008) and GeoB 10042-1 and GeoB 10043-3 (Setiawan et al., 2015); e. total cyst concentrations for Core BAR 9403 (Murgese et al., 2008); f. spliced $\delta^{18}\text{O}_{\text{sw}}$ record for the GeoB 10042-1 and GeoB 10043-3 (Setiawan et al., 2015), and Planktonic foraminifera $\delta^{18}\text{O}_{\text{sw}}$ in the southern Makassar cores (dotted curve) and West Pacific cores (solid curve) (Linsley et al., 2010); g. the difference in $\delta^{18}\text{O}$ of calcite between the annual-mean and winter ($\Delta\delta^{18}\text{O}$) (Mohtadi et al., 2011); h. Core MD78 (near Sumba Indonesia) *Pulleniatina obliquiloculata* Mg/Ca upper thermocline temperatures (80–120 m) (Linsley et al., 2010); i. the June insolation at 30°N (Berger and Loutre, 1991); and j. reconstructed sea level fluctuation of the Sunda Shelf (Hanebuth et al., 2011).

increased paleoproductivity associated with additional input of terrigenous materials. Owing to the southward migration of the Intertropical Convergence Zone, the large amounts of moisture were carried to the EIO and caused heavy rainfall over the region during the northwest monsoon season (Qu et al., 2005). Fukumoto et al. (2015) proposed that the wettest climate from 3.1 ka BP to the present may reflect increased importance of an austral hemisphere atmospheric convection and subsequent southerly position of the Intertropical Convergence Zone at austral summer time. Therefore, we suggest that the changes in the BSi in late Holocene document the rise in the terrigenous inputs, triggering the dramatic increase in clastic sedimentation as well as increased nutrient loading and aquatic primary productivity. The variations of paleoproductivity in Core CJ01-185 during the early Holocene were influenced by the opening of the Sunda Strait at approximately 10 ka. The sedimentation rates recorded in sediments of Core CJ01-185 increased significantly from 6.5 cm/ka during the last glacial period to 20 cm/ka in the Holocene (Xu et al., 2017), which could be associated to the additional input of terrigenous nutrients from the Java Sea into the EIO after the opening of the Sunda Strait at approximately 10 ka. Terrigenous materials with high kaolinite content from the Java Sea were transported into the EIO through the Sunda Strait during the Holocene (Gingele et al., 2002). Mohtadi et al. (2011) indicated that the opening of the Sunda Strait at approximately 10 ka was a major control on paleoproductivity records, as the fresher Java Sea waters and the resulting freshwater cap introduced into the eastern tropical Indian Ocean reduced local upwelling intensity during the Holocene. Murgese et al. (2008) did not identify obvious and persistent upwelling conditions offshore Sumatra for the last 35 000 a.

6 Conclusions

The 20 000 a record of the biogenic silica flux from the eastern India Ocean off the Sunda Strait reflects changes in the primary productivity and provides information regarding changes of the paleoproductivity evolution before and after the opening of the Sunda Strait. The BSi content of Core CJ01-185 showed lowest 0.86% in the last glacial period, and reached its higher value of 1.89% in the late Holocene. Furthermore, the MAR_{BSi} values also varied with much higher during the late Holocene than during the last glacial period. The paleoproductivity in the study area was dominated by the southeast monsoon and the upwelling before the opening of the Sunda Strait. However, the paleoproductivity was mainly controlled by the terrigenous materials input after the opening of the Sunda Strait, and the effects of the southeast monsoon and the upwelling were relatively weak.

Acknowledgments

We would like to thank the crew of R/V *Geomarin III* for their help with sampling on board. Thanks to Director of Marine Research Center, the Agency of Research and Human Resources for Marine and Fisheries of the Ministry of Marine Affairs and Fisheries of the Republic of Indonesia (KKP); Director of the Marine Geological Institute of Indonesia, the Ministry of Energy and Mineral Resources (KESDM); and Director of the Research Center for Geotechnology, Indonesia Institute of Science (LIPI) for their support of joint study.

References

Bergamaschi B A, Tsamakis E, Keil R G, et al. 1997. The effect of grain size and surface area on organic matter, lignin and carbo-

- hydrate concentration, and molecular compositions in Peru Margin sediments. *Geochimica et Cosmochimica Acta*, 61(6): 1247–1260, doi: [10.1016/S0016-7037\(96\)00394-8](https://doi.org/10.1016/S0016-7037(96)00394-8)
- Berger A, Loutre M F. 1991. Insolation values for the climate of the last 10 million years. *Quaternary Science Reviews*, 10: 297–317, doi: [10.1016/0277-3791\(91\)90033-Q](https://doi.org/10.1016/0277-3791(91)90033-Q)
- Bernárdez P, Prego R, Francés G, et al. 2005. Opal content in the Ría de Vigo and Galician continental shelf: biogenic silica in the muddy fraction as an accurate paleoproductivity proxy. *Continental Shelf Research*, 25: 1249–1264, doi: [10.1016/j.csr.2004.12.009](https://doi.org/10.1016/j.csr.2004.12.009)
- De Wever P, Dumitrica P, Caulet J P, et al. 2002. *Radiolarians in the Sedimentary Record*. Boca Raton, FL: CRC Press
- DeMaster D J. 1981. The supply and accumulation of silica in the marine environment. *Geochimica et Cosmochimica Acta*, 45: 1715–1732, doi: [10.1016/0016-7037\(81\)90006-5](https://doi.org/10.1016/0016-7037(81)90006-5)
- DeMaster D J. 1991. Measuring biogenic silica in marine sediments and suspended matter. In: Hurd D C, Spenser D W, eds. *Marine Particles: Analysis and Characterization*. Washington, DC: American Geophysical Union, 363–368
- Fukumoto Y, Li X, Yasuda Y, et al. 2015. The Holocene environmental changes in southern Indonesia reconstructed from highland caldera lake sediment in Bali Island. *Quaternary International*, 374: 15–33, doi: [10.1016/j.quaint.2015.03.020](https://doi.org/10.1016/j.quaint.2015.03.020)
- Gingele F X, De Deckker P, Girault A, et al. 2002. History of the South Java Current over the past 80 ka. *Palaeogeography, Palaeoclimatology, Palaeoecology*, 183(3–4): 247–260
- Gordon A L. 2005. Oceanography of the Indonesian seas and their throughflow. *Oceanography*, 18(4): 14–27, doi: [10.5670/oceanog](https://doi.org/10.5670/oceanog)
- Gordon A L, Susanto R D, Vranes K. 2003. Cool Indonesian throughflow as a consequence of restricted surface layer flow. *Nature*, 425: 824–828, doi: [10.1038/nature02038](https://doi.org/10.1038/nature02038)
- Hanebuth T, Statterger K, Grootes P M. 2000. Rapid flooding of the Sunda Shelf: a late-glacial sea-level record. *Science*, 288: 1033–1035, doi: [10.1126/science.288.5468.1033](https://doi.org/10.1126/science.288.5468.1033)
- Hanebuth T J J, Voris H K, Yokoyama K, et al. 2011. Formation and fate of sedimentary depocentres on Southeast Asia's Sunda Shelf over the past sea-level cycle and biogeographic implications. *Earth Science Reviews*, 104: 92–110, doi: [10.1016/j.earscirev.2010.09.006](https://doi.org/10.1016/j.earscirev.2010.09.006)
- Karleskint G Jr, Turner R, Small J W Jr. 2012. *Introduction to Marine Biology*. 4th ed. US: Cengage Learning
- Levitus S, Boyer T P. 1994. *World Ocean Atlas 1994*. Washington, DC: U. S. Department of Commerce
- Lin S, Hsieh I J, Huang K M, et al. 2002. Influence of the Yangtze River and grain size on the spatial variations of heavy metals and organic carbon in the East China Sea continental shelf sediments. *Chemical Geology*, 182: 377–394, doi: [10.1016/S0009-2541\(01\)00331-X](https://doi.org/10.1016/S0009-2541(01)00331-X)
- Linsley B K, Rosenthal Y, Oppo D W. 2010. Holocene evolution of the Indonesian throughflow and the western Pacific warm pool. *Nature Geoscience*, 3: 578–583, doi: [10.1038/ngeo920](https://doi.org/10.1038/ngeo920)
- Lückge A, Mohtadi M, Rühlemann C, et al. 2009. Monsoon versus ocean circulation controls on paleoenvironmental conditions off southern Sumatra during the past 300,000 years. *Paleoceanography*, 24: PA1208, doi: [10.1029/2008PA001627](https://doi.org/10.1029/2008PA001627)
- Mohtadi M, Oppo D W, Steinke S, et al. 2011. Glacial to Holocene swings of the Australian-Indonesian monsoon. *Nature Geoscience*, 4: 540–544, doi: [10.1038/ngeo1209](https://doi.org/10.1038/ngeo1209)
- Mortlock R A, Froelich P N. 1989. A simple method for the rapid determination of biogenic opal in pelagic marine sediments. *Deep-Sea Research Part A. Oceanographic Research Papers*, 36: 1415–1426, doi: [10.1016/0198-0149\(89\)90092-7](https://doi.org/10.1016/0198-0149(89)90092-7)
- Murgese D S, De Deckker P, Spooner M I, et al. 2008. A 35,000 year record of changes in the eastern Indian Ocean offshore Sumatra. *Palaeogeography, Palaeoclimatology, Palaeoecology*, 265: 195–213, doi: [10.1016/j.palaeo.2008.06.001](https://doi.org/10.1016/j.palaeo.2008.06.001)
- Nelson D M, Tréguer P, Brzezinski M A, et al. 1995. Production and dissolution of biogenic silica in the ocean: Revised global estimates, comparison with regional data and relationship to biogenic sedimentation. *Global Biogeochemical Cycles*, 9(3):

- 359–372, doi: [10.1029/95GB01070](https://doi.org/10.1029/95GB01070)
- Qu Tangdong, Du Yan, Strachan J, et al. 2005. Sea surface temperature and its variability in the Indonesian region. *Oceanography*, 18: 50–61, doi: [10.5670/oceanog](https://doi.org/10.5670/oceanog)
- Ragueneau O, Leynaert A, Tréguer P, et al. 1996. Opal studied as a marker of paleoproductivity. *EOS*, 77: 491
- Ragueneau O, Tréguer P, Leynaert A, et al. 2000. A review of the Si cycle in the modern ocean: recent progress and missing gaps in the application of biogenic opal as a paleoproductivity proxy. *Global and Planetary Change*, 26: 317–365, doi: [10.1016/S0921-8181\(00\)00052-7](https://doi.org/10.1016/S0921-8181(00)00052-7)
- Romero O E, Mohtadi M, Helmke P, et al. 2012. High interglacial diatom paleoproductivity in the westernmost Indo-Pacific Warm Pool during the past 130,000 years. *Paleoceanography*, 27: PA3209, doi: [10.1029/2012PA002299](https://doi.org/10.1029/2012PA002299)
- Romero O E, Rixen T, Herunadi B. 2009. Effects of hydrographic and climatic forcing on diatom production and export in the tropical southeastern Indian Ocean. *Marine Ecology Progress Series*, 384: 69–82, doi: [10.3354/meps08013](https://doi.org/10.3354/meps08013)
- Schoepfer S D, Shen J, Wei H Y, et al. 2015. Total organic carbon, organic phosphorus, and biogenic barium fluxes as proxies for paleomarine productivity. *Earth Science Reviews*, 149: 23–52, doi: [10.1016/j.earscirev.2014.08.017](https://doi.org/10.1016/j.earscirev.2014.08.017)
- Setiawan R Y, Mohtadi M, Southon J, et al. 2015. The consequences of opening the Sunda Strait on the hydrography of the eastern tropical Indian Ocean. *Paleoceanography*, 30: 1358–1372, doi: [10.1002/2015PA002802](https://doi.org/10.1002/2015PA002802)
- Sprintall J, Gordon A L, Koch-Larrouy A, et al. 2014. The Indonesian seas and their role in the coupled ocean-climate system. *Nature Geoscience*, 7(7): 487–492, doi: [10.1038/ngeo2188](https://doi.org/10.1038/ngeo2188)
- Sprintall J, Wijffels S, Molcard R, et al. 2010. Direct evidence of the South Java Current system in Ombai Strait. *Dynamics of Atmospheres and Oceans*, 50: 140–156, doi: [10.1016/j.dynatmoce.2010.02.006](https://doi.org/10.1016/j.dynatmoce.2010.02.006)
- Susanto R D, Gordon A L, Zheng Quanan. 2001. Upwelling along the coasts of Java and Sumatra and its relation to ENSO. *Geophysical Research Letters*, 28: 1599–1602, doi: [10.1029/2000GL011844](https://doi.org/10.1029/2000GL011844)
- Talley L D, Sprintall J. 2005. Deep expression of the Indonesian Throughflow: Indonesian intermediate water in the South Equatorial Current. *Journal of Geophysical Research: Oceans*, 110(C10): doi: [10.1029/2004JC002826](https://doi.org/10.1029/2004JC002826)
- Wang Liang, Fan Dejiang, Li Weiran, et al. 2014. Grain-size effect of biogenic silica in the surface sediments of the East China Sea. *Continental Shelf Research*, 81: 29–37, doi: [10.1016/j.csr.2014.03.005](https://doi.org/10.1016/j.csr.2014.03.005)
- Wang Yonghong, Yu Zhigang, Li Guanxue, et al. 2009. Discrimination in magnetic properties of different-sized sediments from the Changjiang and Huanghe Estuaries of China and its implication for provenance of sediment on the shelf. *Marine Geology*, 260: 121–129, doi: [10.1016/j.margeo.2009.02.008](https://doi.org/10.1016/j.margeo.2009.02.008)
- Xu Jian, Holbourn A, Kuhnt W, et al. 2008. Changes in the thermocline structure of the Indonesian outflow during Terminations I and II. *Earth and Planetary Science Letters*, 273: 152–162, doi: [10.1016/j.epsl.2008.06.029](https://doi.org/10.1016/j.epsl.2008.06.029)
- Xu Yonghang, Wang Liang, Yin Xijie, et al. 2017. The influence of the Sunda Strait opening on paleoenvironmental changes in the eastern Indian Ocean. *Journal of Asian Earth Sciences*, 146: 402–411, doi: [10.1016/j.jseaes.2017.06.014](https://doi.org/10.1016/j.jseaes.2017.06.014)
- Zhao Yue, Ding Xuan. 2011. Sedimentary record and monsoon activity of core BAR9442 in Sunda Strait during 30 ka BP. *Earth Science-Journal of China University of Geosciences (in Chinese)*, 36(4): 610–620